

UNCLASSIFIED

AD NUMBER

AD026307

LIMITATION CHANGES

TO:

Approved for public release; distribution is unlimited.

FROM:

Distribution authorized to U.S. Gov't. agencies and their contractors;
Administrative/Operational Use; SEP 1953. Other requests shall be referred to Office of Naval Research, Washington, DC.

AUTHORITY

onr ltr, 9 nov 1977

THIS PAGE IS UNCLASSIFIED

Armed Services Technical Information Agency

AID

PLEASE RETURN THIS COPY TO:

ARMED SERVICES TECHNICAL INFORMATION AGENCY
DOCUMENT SERVICE CENTER
Knott Building, Dayton 2, Ohio

Because of our limited supply you are requested to return this copy as soon as it has served your purposes so that it may be made available to others for reference use. Your cooperation will be appreciated.

26307

NOTICE: WHEN GOVERNMENT OR OTHER DRAWINGS, SPECIFICATIONS OR OTHER DATA ARE USED FOR ANY PURPOSE OTHER THAN IN CONNECTION WITH A DEFINITELY RELATED GOVERNMENT PROCUREMENT OPERATION, THE U. S. GOVERNMENT THEREBY INCURS NO RESPONSIBILITY, NOR ANY OBLIGATION WHATSOEVER; AND THE FACT THAT THE GOVERNMENT MAY HAVE FORMULATED, FURNISHED, OR IN ANY WAY SUPPLIED THE SAID DRAWINGS, SPECIFICATIONS, OR OTHER DATA IS NOT TO BE REGARDED BY IMPLICATION OR OTHERWISE AS IN ANY MANNER LICENSING THE HOLDER OR ANY OTHER PERSON OR CORPORATION, OR CONVEYING ANY RIGHTS OR PERMISSION TO MANUFACTURE, USE OR SELL ANY PATENTED INVENTION THAT MAY IN ANY WAY BE RELATED THERETO.

Reproduced by
DOCUMENT SERVICE CENTER
KNOTT BUILDING, DAYTON, 2, OHIO

UNCLASSIFIED

THIS REPORT HAS BEEN DELIMITED
AND CLEARED FOR PUBLIC RELEASE
UNDER DOD DIRECTIVE 5200.20 AND
NO RESTRICTIONS ARE IMPOSED UPON
ITS USE AND DISCLOSURE.

DISTRIBUTION STATEMENT A

APPROVED FOR PUBLIC RELEASE;
DISTRIBUTION UNLIMITED.

University of California
College of Engineering
Submitted under Contract Nonr 222(17)
with the Office of Naval Research

Institute of Engineering Research
Wave Research Laboratory

Series 74 Issue 7

DEPTH DETERMINATION ON BEACHES BY WAVE VELOCITY

METHODS

by

R. A. Fuchs

Berkeley, California
September 1953.

DEPTH DETERMINATION ON BEACHES BY WAVE VELOCITY METHODS.

by
R. A. Fuchs

Introduction

During World War II extensive applications were made of methods for determining water depths adjacent to ocean beaches by analyses of timed aerial photographs of the waves approaching the shore. Since the bottom slopes found off sandy coasts are usually small, the observable wave characteristics were related to the water depth, h , by the formula,

$$C = \frac{L}{T} = \left(\frac{g L}{2 \pi} \tanh \frac{2 \pi h}{L} \right)^{1/2}, \quad (1)$$

valid for small amplitude sinusoidal waves of wavelength L and period T , and velocity C in water of constant depth.

Even a cursory examination of ocean waves, however, will reveal a complex pattern which is rarely similar to the idealized wave for which Equation (1) is valid. For this reason alone one would expect appreciable differences between computed and sounded depths. Such differences do occur in practice and in the present report we shall investigate to what extent this might be due to a departure from the idealized conditions.

Complex Wave Systems

Assume that for the region and time of interest the irregular ocean surface can be represented by the sum of sinusoidal waves of suitable amplitude, period, phase and direction of motion for each of which Equation (1) is valid. Since each of the waves travels with a velocity determined by its period and the depth of water, a resultant wave crest continually deforms as it moves. The term wave velocity applied to such a crest will be interpreted to mean the horizontal velocity of the relative maximum of the surface profile. It may be impossible to distinguish this relative maximum exactly in aerial photographs and a different definition of wave velocity might be preferred. This would be of some importance for relatively flat crests for which the crest position shifts rapidly. Horizontal (terrestrial) photographs of wave velocities may be erratic for this reason, as observed in data obtained for ocean waves by Moffitt^{(1)*} and for laboratory waves by Sibul⁽²⁾.

The velocity of propagation of a sinusoidal wave of small steepness is practically independent of wave amplitude. In a complex wave system, however, the crest velocity depends strongly on the individual wave amplitudes as we shall see. Since stereophotography is generally considered to be too complex for depth determinations, it would then appear that the accurate analysis of aerial photographs for water depths must always be doomed to failure. We shall see, however, that certain waves may furnish better results than others.

* Numbers in parentheses refer to references listed at the end of this report.

The essential ideas involved can be exhibited by considering the sum of two sinusoidal waves of different amplitudes and periods. We assume that the waves are long-crested and travel in the same direction in water of constant depth. The argument involved is essentially the same for any finite number of component waves with a single exception, which will be noted. The surface elevation at time t and at a distance x from a fixed vertical is assumed to be given by

$$\eta(x, t) = a \cos(kx - \sigma t) + b \cos(lx - \gamma t + \phi) \quad (2)$$

where a and b are constant amplitudes of the components, $\sigma^2 = gk \tanh kh$, ϕ is a constant phase angle and h is the water depth. Crests are located at points x_0 for which $\frac{\partial \eta(x_0, t)}{\partial x} = 0$, $\frac{\partial^2 \eta(x_0, t)}{\partial x^2} < 0$, i.e.,

$$\frac{\partial \eta(x_0, t)}{\partial x} = a k \sin(kx_0 - \sigma t) + b l \sin(lx_0 - \gamma t + \phi) = 0 \quad (3)$$

$$-\frac{\partial^2 \eta(x_0, t)}{\partial x^2} = a k^2 \cos(kx_0 - \sigma t) + b l^2 \cos(lx_0 - \gamma t + \phi) > 0. \quad (4)$$

From the implicit relation (3), defining x_0 as a function of t , the horizontal crest velocity $\frac{dx_0}{dt}$ is found to be,

$$C = \frac{dx_0}{dt} = - \frac{\frac{\partial^2 \eta(x_0, t)}{\partial x \partial t}}{\frac{\partial^2 \eta(x_0, t)}{\partial x^2}} = \frac{a k \sigma \cos(kx_0 - \sigma t) + b l \gamma \cos(lx_0 - \gamma t + \phi)}{a k^2 \cos(kx_0 - \sigma t) + b l^2 \cos(lx_0 - \gamma t + \phi)}.$$

Notice that if $b=0$, $a \neq 0$, the wave motion is sinusoidal and the wave velocity is $C = \sigma/k = L_1/T_1$ where L_1 and T_1 are the wavelength and period of the wave, respectively. This velocity is independent of the wave amplitude a and verifies Equation (1) for a single sinusoidal wave. In general we see that C depends on the ratio of component amplitudes and is a complex function of x and t as well.

Let us assume that of the two component velocities $C_1 = \sigma/k$ and $C_2 = \gamma/l$, C_1 is the larger. Then one easily verifies, by cross multiplication, that at crest positions for which the second component wave with velocity C_2 is above the still water level $C < C_1$, while at crests for which the first component is positive $C_2 < C$. Now one will usually encounter the highest waves in a complex wave system when the component waves constructively reinforce each other, i.e., both $\eta_1 = a \cos(kx - \sigma t)$ and $\eta_2 = b \cos(lx - \gamma t + \phi)$ are positive. For such crests we then have $C_2 < C < C_1$. This constructive reinforcement at crests is illustrated in Figure 1 by several examples taken from a report by Mathewson⁽³⁾. If one finds, for example, periods of 10 to 12 seconds one would expect the crest velocities of the high waves to fall in the small interval between the velocities of the 10 and 12 second period waves. Small crests do not necessarily satisfy the conditions that both components are positive and hence their velocities may fall far outside of the interval $C_2 < C < C_1$. One can, by a suitable choice of amplitude ratio, periods, and depth of water, obtain crests whose velocities at some instant vanish. Such phenomena have been observed in the laboratory for very flat crests. Similar results are possible for three or more component waves. If the largest velocity of a component is C_1 and the smallest C_2 , then for crests at which all components constructively reinforce each other $C_2 < C < C_1$.

In order to illustrate these results we consider two sinusoidal waves of equal amplitude with periods of 5.23 and 5.86 seconds in 20 feet of water. The corresponding wavelengths are 116 and 131 feet and the wave velocities 21.7 and 22.3 ft./sec., respectively. The resultant surface profile is plotted in Figure 2 for five instants 2.88 seconds apart. The crest velocity, C , is obtained by dividing the distance traveled by a crest between successive graphs by 2.88 seconds. The wave length, L at a crest position is linearly interpolated, i.e., $L = \frac{2L_1L_2}{L_1 + L_2}$ where L_1 and L_2 are measured wave lengths on either side of the crest considered at the given instant. The period T is taken as an average of periods before and after the instant considered. Using L and C , Crest (2) in Figure 2 was found to give depths of 23.5, 23.0, 22.2 and 19.0 feet for times, t , of -5.76, -2.88, 0, 2.88 seconds, respectively; Crest (3) gives depths of 22.5 and 26.0 feet for $t = 0, 2.88$ seconds; Crest (4) gives a depth of 18.1 feet for $t = 0$. It was found that if crests are chosen whose amplitudes are larger than $1/10$ of their maximum values, the computed depth is within 10 percent of the correct depth. One sees, however, that considerable scatter of computed depths results from using small waves.

In a complex wave system the term wave period loses its usual significance. Although it is possible to accurately measure a crest velocity, the period to be associated with it may be subject to considerable uncertainty. If the period is sufficiently large for a fixed depth, this depth may be calculated rather accurately, as illustrated in Figure 3, since the depth is relatively insensitive to period changes. As a wave approaches shallow water, C approaches \sqrt{gh} , a result independent of period. It is important to note that this latter equation can be derived quite independently of Equation (1), without the assumption of periodicity. One would therefore expect that good results can be had in depth analysis if long period waves are used, and that poorer results will generally result from use of short period waves. To illustrate this point, we have plotted in Figure 3 several points taken from an analysis of aerial photographs of ocean waves by Moffitt⁽⁴⁾. Since the depth rapidly changes with period in the immediate neighborhood of some of these points, one would expect to find relatively large errors in computed depth there, and this proves to be the case.

Since the spread of velocities is greater in deep water than in shallow water for the same spread of periods, waves in deep water are more irregular than in shallow water. Irregular waves in deep water rapidly deform as they move, eventually disappearing completely. To illustrate this lack of permanence of wave form and its dependence on depth, consider a wave system formed by adding two sinusoidal waves of periods 8 and 12 seconds. The velocities of these waves in several water depths are tabulated below:

| h | | 20' | 50' | 100' |
|--------------|-------------|-----|-----|------|
| C ft/sec. | T = 8 sec. | 23 | 33 | 39 |
| | T = 12 sec. | 24 | 37 | 48 |

We see that in 100 feet of water the component crests rapidly separate and a crest may well disappear. On the other hand, in 50 feet of water the difference of velocities is so small that a crest preserves its identity until it breaks. A large fixed degree of deformation of a crest will occur when the larger period wave moves, relative to the smaller, one half of the wave length

of the smaller period wave. For $h = 100$ feet the elapsed time is 17 sec., corresponding to a travel distance of 825 ft. For $h = 50$ feet, the time is 36 sec. and the travel distance 1360 ft. For $h = 20$ feet the time is 105 sec. and the distance is 2300 ft. Thus it appears quite likely that ocean waves will preserve their identity on a beach from say 50 feet depth up to the point of breaking. It will be relatively easy to follow crests in shallow water and the problem of depth determination is thereby simplified.

Fourier Analysis

In view of the fact, just demonstrated, that the water depth can not be determined exactly from an analysis of timed aerial photographs of complex waves, it is of interest to see if the exact determination is possible if complete data are available. For this purpose irregular waves were generated by manual operation of the wave flapper in the laboratory wave channel and continuous readings of surface elevation were made at two points 3.47 feet apart in water of constant depth 2.21 feet. Let us assume that a wave record, as a function of time, t , is given over the finite interval $-T < t < T$ and can therefore be represented in this interval by the Fourier series

$$\eta(x, t) = \frac{a_0}{2} + \sum_{s=1}^{\infty} a_s \cos \frac{s \pi t}{T} + b_s \sin \frac{s \pi t}{T}$$

where

$$a_s = \frac{1}{T} \int_{-T}^T \eta(x, t) \cos \frac{s \pi t}{T} dt, \quad b_s = \frac{1}{T} \int_{-T}^T \eta(x, t) \sin \frac{s \pi t}{T} dt.$$

This equation for η can also be written in the form

$$\eta(x, t) = \frac{a_0}{2} + \sum_{s=1}^{\infty} \sqrt{a_s^2 + b_s^2} \cos \left(\frac{s \pi t}{T} - \phi_s \right)$$

where $\tan \phi_s = b_s / a_s$. In this form we see that $\phi_s = k_s x + \theta_s$, where k_s is the wave number $2\pi/L_s$ corresponding to the period $T/2s$, and θ_s is the phase of this component at $t = 0$, $x = 0$. By Fourier analysis we find both b_s and a_s and hence ϕ_s for two different values of x . Subtracting we get $k_s D$, D being the horizontal distance between elements which is 3.47 ft. in our case. From this we can compute the water depth since the period $T/2s$ is known.

This process was applied to a finite wave train which lasted for 13.5 sec. (see Figure 4). For a component wave having a period of 1.5 seconds the computed depth was 2.18 feet. Of course many more waves would have to be analyzed before definite statements as to the success of the method could be made. However, it appears likely on the basis of this single example that the depth can be computed if one has complete information. Unfortunately this information is lacking in the data usually gathered for depth determination purposes.

Wave Crest Velocities on a Sloping Beach

In deep water the crest velocity is independent of depth and therefore independent of bottom slope. The effect of depth on the velocity increases

as the depth decreases, being largest in the very shallow water. We shall, therefore, investigate the effect of beach slope on crest velocity in shallow water, and if it is negligibly small here it will also be negligible in deeper water.

Explicit formulae are available for describing the motion of small amplitude shallow water waves on a beach of constant slope⁽⁵⁾. Progressive waves traveling toward shore with crests parallel to the shore line have a surface profile which can be expressed in terms of the regular and singular Bessel functions J_0 and Y_0 in the form

$$\eta(x, t) = A \left[\cos(\sigma t - \epsilon) Y_0(z) + \sin(\sigma t - \epsilon) J_0(z) \right]$$

where $z = 2\sqrt{\frac{mx}{q}}$, q is the beach slope, ϵ the phase angle, A the constant amplitude factor, $m = \sigma^2/g$, $\sigma = 2\pi/T$, T is the wave period and x is the horizontal distance measured out from the shore line. If we denote x_0 the x -value of a wave crest, then $\frac{\partial \eta}{\partial x}(x_0, t) = 0$, or

$$\cos(\sigma t - \epsilon) Y_0'(z_0) + \sin(\sigma t - \epsilon) J_0'(z_0) = 0,$$

the prime denoting differentiation with respect to the argument z and $z_0 = 2\sqrt{\frac{mx_0}{q}}$. This equation defines x_0 implicitly as a function of t . Thus the crest velocity is

$$\begin{aligned} V_c &= -\frac{dx_0}{dt} = \frac{\frac{\partial^2 \eta(x_0, t)}{\partial x \partial t}}{\frac{\partial^2 \eta(x_0, t)}{\partial x^2}} = \frac{\sigma}{\sqrt{\frac{m}{q} x_0}} - \frac{\sin(\sigma t - \epsilon) Y_0'(z_0) + \cos(\sigma t - \epsilon) J_0'(z_0)}{\cos(\sigma t - \epsilon) Y_0''(z_0) + \sin(\sigma t - \epsilon) J_0''(z_0)} \\ &= \sqrt{gh} \frac{J_0'^2(z_0) + Y_0'^2(z_0)}{J_0'(z_0) Y_0''(z_0) - J_0''(z_0) Y_0'(z_0)}. \end{aligned}$$

Employing some identities for Bessel functions (see (6), p. 76) this can be written in the form

$$V_c = \sqrt{gh} (J_1^2(z_0) + Y_1^2(z_0)) \frac{\pi z_0}{2}.$$

For large z_0 we have approximately (see (6), p. 224)

$$\begin{aligned} V_c &= \sqrt{gh} \sum_{m=0}^{\infty} \left\{ 1 \cdot 3 \cdot 5 \cdots (2m-1) \right\} \frac{(1, m)}{2^m z_0^{2m}} \\ &= \sqrt{gh} \left\{ 1 + \frac{1 \cdot 3}{2z_0^2 \cdot 2^2 \cdot 1!} - \frac{1 \cdot 3 \cdot 3 \cdot 5}{2^2 \cdot z_0^4 \cdot 2^4 \cdot 2!} + \cdots \right\} \end{aligned}$$

where $(1, 0) = 1$ $(1, m) = \frac{(4-1^2)(4-3^2)\cdots(4-(2m-1)^2)}{2^{2m} m!}$ for $m > 0$.

The remainder after p terms in this series is of the same sign as, and numerically less than, the $p+1$ -th term. Therefore, the error involved in the use of \sqrt{gh} as an approximation for V_c is

$$\begin{aligned} \Delta V_c &= \frac{V_c - \sqrt{gh}}{\sqrt{gh}} = \frac{3}{32} \left\{ \frac{q}{mx_0} - \frac{15}{64} \left(\frac{q}{mx_0} \right)^2 + \cdots \right\} \\ &= \frac{3}{32} \left\{ \frac{g}{h} \left(\frac{q}{\sigma} \right)^2 - \frac{15}{64} \left(\frac{g}{h} \right)^2 \left(\frac{q}{\sigma} \right)^4 + \cdots \right\}. \end{aligned}$$

To take a somewhat extreme case for depth determination, consider $T = 10$ sec., $h = 10$ ft., $q = 1/10$. Then $\Delta V_0 = 0.77 - 0.14 + \dots$ percent. If $q = 1/5$ and still $T = 10$ sec., $h = 10$ ft., then $\Delta V_0 = 3.06 - 2.34 + \dots$ percent. We see that for beaches with slopes less than $1/10$ the effect of slope is very small and begins to be appreciable for slopes of about $1/5$.

For slopes larger than about $1/10$ for which the series approximation is no longer rapidly convergent, we write V_0 in terms of the Bessel function

$$H_1^{(1)}(x). \quad \text{Since} \quad H_1^{(1)}(x) = J_1(x) + iY_1(x),$$

$$V_0 = \sqrt{gh} \frac{\pi z_0}{2} |H_1^{(1)}(z_0)|^2$$

$$\text{and} \quad \Delta V_0 = \frac{\pi z_0}{2} |H_1^{(1)}(z_0)|^2 - 1,$$

which is plotted in Figure 5. In this graph we find that for $T = 10$ sec., $h = 10$ ft. and $q = 1/5$, $\Delta V_0 = 2.8$ percent while if $q = 1/10$, $T = 10$ sec., $h = 10$ ft., $\Delta V_0 = 0.73$ percent. Since the error in depth is approximately twice the error in crest velocity, the errors in depth in these cases are about 5.6 percent and 1.5 percent, respectively. This is still small if one is interested in depths to within one foot, as is usually the case for amphibious landings.

Wave Lengths on a Sloping Bottom

A uniform wave train progressing towards shore has a constant period independent of water depths and a crest velocity which is nearly \sqrt{gh} , as we have just seen. However, the wave length to be associated with the measured period and velocity is not directly measurable, for the distance between crests varies continuously with depth. A method of graphical integration has been proposed by Johnson (7) for obtaining the observed wave lengths on a beach. Such calculations can be performed numerically in a somewhat different form as we now show.

Let x be the horizontal distance measured in the direction of wave travel directly toward shore with origin at the "deep water point" for which $h/5.12T^2 = 0.5$. The bottom profile will be described by its Taylor series expansion

$$x_0 - x = a_1 h + a_2 h^2 + \dots$$

where x_0 is the distance from shore to deep water. Assuming that the bottom slope is sufficiently small, the instantaneous wave velocity is

$$C = \frac{dx}{dt} = \frac{L}{T} = \frac{\sigma}{k} = \frac{gT}{2\pi} \tanh \frac{2\pi h}{CT}$$

where L is here a fictitious instantaneous wave length.

Consider a wave whose surface profile has the form

$$\eta(x, t) = a(x) \cos(\phi(x) - \sigma t)$$

where $a(x)$ is a slowly varying function of x . In analogy to the interpretation

of c for constant depth, we define the wave velocity in the general case as

$$C = \frac{\sigma}{\frac{\partial \phi}{\partial x}} = \frac{\sigma}{k}.$$

Thus $\frac{\partial \phi}{\partial x} = k = \frac{2\pi}{L}$ or $\phi = \int_0^x k dx + \text{constant}.$

We choose the constant to be zero which amounts to choosing the phase as zero when $x = 0$ and $t = 0$. Thus,

$$\begin{aligned} -\frac{\phi}{2\pi} &= \frac{1}{2\pi} \int_{h_0}^h (a_1 + 2a_2 h + \dots) k dh \\ &= a_1 \int_{1/2}^{\frac{h}{L_0}} \frac{d(\frac{h}{L_0})}{\frac{L}{L_0}} + 2a_2 L_0 \int_{1/2}^{\frac{h}{L_0}} \frac{\frac{h}{L_0} d(\frac{h}{L_0})}{\frac{L}{L_0}} + \dots \end{aligned}$$

where $\frac{h_0}{5.12 T^2} = 0.5$.

If we denote by

$$S\left(\frac{h}{L_0}\right) = \int_{\frac{1}{2}}^{\frac{h}{L_0}} \frac{d(\frac{h}{L_0})}{\frac{L}{L_0}}, \quad R\left(\frac{h}{L_0}\right) = \int_{\frac{1}{2}}^{\frac{h}{L_0}} \frac{\frac{h}{L_0} d(\frac{h}{L_0})}{\frac{L}{L_0}} = \frac{h}{L_0} S\left(\frac{h}{L_0}\right) + \int_{\frac{1}{2}}^{\frac{h}{L_0}} S\left(\frac{h}{L_0}\right) d\left(\frac{h}{L_0}\right)$$

we have

$$\frac{\phi}{2\pi} = a_1 S\left(\frac{h}{L_0}\right) + 2a_2 L_0 R\left(\frac{h}{L_0}\right) + \dots$$

The quantity $i = \frac{\phi}{2\pi}$, which might be called the wave length index, takes on integral values only at the wave crests for $t = 0$. Hence by computing the integrals as functions of h/L_0 we can determine the crest positions for $t = 0$, or more generally for arbitrary t by subtracting t/T and thus we determine the wave lengths. The functions $S\left(\frac{h}{L_0}\right)$ and $R\left(\frac{h}{L_0}\right)$ are tabulated in Table 1.

If the wave length changes slowly with depth, as for a very flat beach, the integrals can be estimated and we find approximately that the computed wave length is associated with the water depth midway between crests. The crest positions and thus the wave lengths involved can be used together with the assumed period to compute a depth from the equation

$$\frac{L}{T} = \frac{g T}{2\pi} \tanh \frac{2\pi h}{L}.$$

This depth can be compared directly with the known depth midway between crests, or by interpolation the wave length at a crest can be compared with the depth there. The latter comparison is made in Table 2 for beach slopes of $1/40$ and $1/100$ and wave periods of 20, 15, 10 and 5 seconds. The actual error in these cases is quite small. There is a noticeable increase in error with increase in beach slope.

A similar calculation has been made for a parabolic beach profile which rather closely fits the profile sounded at Davenport, California (Figure 6). In Table 3 the computed depth is compared with the depth beneath a crest for wave periods of 20, 15, 10 and 5 seconds. The error increases rapidly with

depth, reflecting the rapid increase of the quadratic term in the equation of the beach profile. Recalling, however, that in the actual case of the Davenport beach the agreement between the parabola and the sounded profile is reasonably good only over the depth range of 0 to 40 feet, the final agreement is quite good.

Short-crested Waves

Waves are called short-crested when their height varies transversely to their direction of propagation. Long-crested waves on the other hand have long straight crests characteristic of swell from a distant storm. It is found that winds blowing in a single direction can raise short-crested waves traveling in this direction. Since all ocean waves are more or less short-crested it is customary to reserve the name short-crested for waves for which the distance between consecutive heights is of the same order of magnitude in any direction. The motion of periodic short-crested waves has been investigated by the author (8) in some detail, beginning with the hydrodynamic equations. For waves of small steepness a periodic short-crested wave can be represented as the sum of two periodic long-crested waves intersecting at an angle, both waves having the same height and period. Thus a simple derivation of the wave velocity formula is made possible by basing it on the formula for long-crested waves.

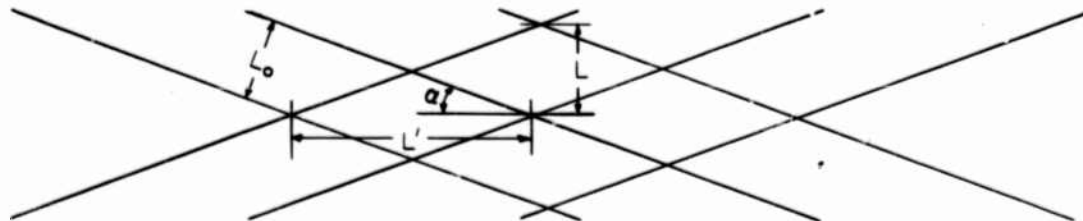
To a first approximation, for which the waveheight to wavelength ratio is small, the surface elevation of a short-crested wave can be written in the form

$$\eta(x, y, t) = a \cos\left(\frac{2\pi}{L}x - \frac{2\pi t}{T}\right) \cos\frac{2\pi}{L'}y$$

where x, y are horizontal coordinates measured in the direction of and perpendicular to the direction of propagation, respectively, L is the wavelength in the direction of travel, L' is the wavelength at right angles to this, T is the wave period, and a is the amplitude. This can be written in the form

$$\eta(x, y, t) = \frac{a}{2} \cos\left(2\pi\left(\frac{x}{L} + \frac{y}{L'}\right) - \frac{2\pi t}{T}\right) + \frac{a}{2} \cos\left(2\pi\left(\frac{x}{L} - \frac{y}{L'}\right) - \frac{2\pi t}{T}\right)$$

which demonstrates that a short-crested wave can be represented as the sum of two long-crested waves. The first long-crested component wave above has crests parallel to the line $y = \frac{L}{L'}x$ while the second has crests parallel to the line $y = -\frac{L}{L'}x$. Let L_0, c_0 and T be the wavelength, velocity and period of one of the long-crested waves, and c and T the velocity and period of the short-crested wave. Denoting by 2α the angle between the two lines of crests, we see from the sketch below



that $L_0 = L \cos \alpha = L' \sin \alpha$. Therefore

$$C = \frac{L}{T} = \frac{L_0}{T} \frac{1}{\cos \alpha} = \frac{C_0}{\cos \alpha}.$$

In water of constant depth, h , the velocity of a long-crested wave is given by

$$C_0^2 = \frac{g L_0}{2 \pi} \tanh \frac{2 \pi h}{L_0} .$$

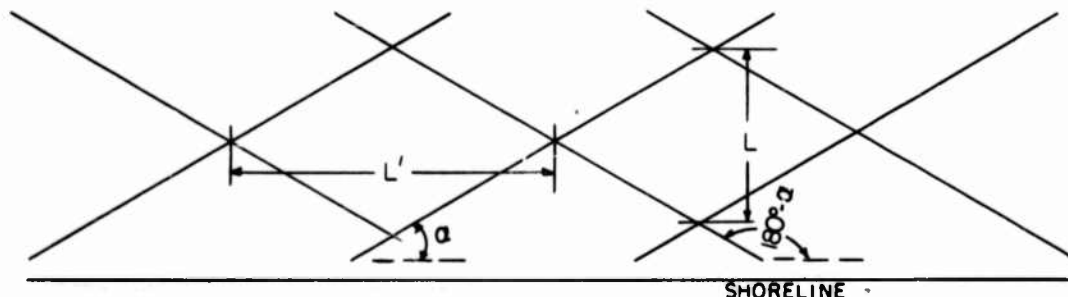
Substituting for C_0 and L_0 in terms of L and L' we find that

$$C^2 = \frac{g L}{2 \pi \cos \alpha} \tanh \frac{2 \pi h}{L \cos \alpha} = \frac{g L}{2 \pi} \sqrt{1 + \left(\frac{L}{L'}\right)^2} \tanh \left(\frac{2 \pi h}{L} \sqrt{1 + \left(\frac{L}{L'}\right)^2} \right)$$

which is the formula derived in an earlier report by the author⁽⁸⁾ directly from the hydrodynamic equations. This formula has been applied by Moffitt⁽⁴⁾ to aerial photographs of waves at Clatsop Spit, Oregon. It appears that for the purpose of depth determination the waves used were practically long-crested although they appear at first sight to be short-crested. It appears from considerations in the following section that in the depths of interest for amphibious operations waves are nearly always long-crested if they have periods larger than about 5 seconds.

Refraction of Short-crested Waves

Short-crested waves can arise on a sloping beach either as the direct result of long-crested waves approaching the beach from different storm areas or by selective refraction of long-crested waves coming from a distant storm area and having a broad frequency spectrum. Consider a regular short-crested wave system made up in deep water of two sinusoidal wave trains which approach the shore line with crests making angles of α and $180^\circ - \alpha$ with this line as shown below



Let L , L' be the wavelengths of the short-crested wave in directions parallel and perpendicular to the shore line, respectively. The ratio L'/L measures the extent to which the waves are short-crested. Waves for which L'/L is near unity are called short-crested while if L'/L is much larger than one the waves are called long-crested. The initial value of the ratio in deep water is $(L'/L) = \cot \alpha_0$, α_0 being the value of α for deep water conditions. Using Snell's law for the refraction and published tables of functions of h/L_0 we have plotted L'/L as a function of h/L_0 and h/L in Figure 7. As an example we find from this graph that a short-crested wave of 13 second period, having $L'/L = 1$ in deep water will have approximately $L'/L = 4$ for $h = 22$ ft. and $L'/L = 6$ for $h = 11$ ft. If we limit the region of interest for depth determination to depths less than 25 feet, the error in depth due to neglecting the short-crested nature of the waves will be of the order of 3 percent

for a 15 second period. These results are in rough agreement with the results presented by Side and Panton (9) who find that short crested waves attain the value $L'/L = 5$ at d/L of about $1/13$.

According to Snell's law the refraction of a wave on a sloping beach depends on the period of the wave and the depth of water as well as on the initial angle of approach. Thus by selective refraction an irregular long-crested wave approaching a beach in a direction other than at normal incidence will be separated into a series of long-crested waves moving in different directions toward the beach. In shallower water the wave pattern will again tend to be long-crested since all component waves tend to align themselves with the shoreline. In Fig. 8 we have plotted the angular divergence, $\Delta \alpha$, of crests for two waves having periods 5 sec. apart beginning with $T = 4.9$ and ending with $T = 10.15$ for initial angles of 50° and 70° . For the shallow depths of direct concern in amphibious operations one sees again that there is little divergence of crests, the waves being nearly long-crested.

Conclusions

These studies result in several important rules for selecting particular waves from a complex wave system whose analysis should lead to improved results in depth determination. It is shown that high waves will probably give more consistent results than low waves in the same system. Long period waves are preferable to short period waves for analysis since the depth is relatively insensitive to period in such cases.

Factors complicating the analysis include the effect of beach slope, short-crested wave patterns, change in form of the wave crests, and continuous variation of wave-length with depth. It is shown that for beach slopes of less than about $1/10$ the crest velocity of small amplitude waves in shallow water is independent of slope and depends only on the depth immediately below a crest. Since the effect of depth decreases as the depth increases, the errors due to neglect of slope in the wave velocity formula should be negligible for slopes less than $1/10$. For these cases the measured wave length can be rather accurately associated with the depth midway between crests, and the wavelength at a crest can be obtained by linear interpolation. Since waves of any sufficiently large period move with the same velocity, \sqrt{gh} , in very shallow water, individual wave crests maintain their identity near shore and thus can be followed for purposes of depth determination. We have seen that crest velocities generally depend on wave amplitudes which are not obtainable directly from the usual aerial photographs. If complete surface time histories are available, the depth could probably be computed exactly as is shown in a single example. Thus the exact analysis is impossible due to lack of sufficient data; but if the suggestions listed above are followed it is believed that sufficiently accurate results can be obtained.

Acknowledgments

I am indebted for many of the calculations to E. O'Keefe. The calculation of wave-length on a sloping beach was performed in part by N. Chien.

References

1. Moffitt, F. H. - Analysis of controlled terrestrial photographs taken at Davenport, California for wave velocity method of depth determination. University of Calif. IER, Series 74, Issue 3, September 1953.
2. Sibul, O. - Laboratory studies of depth determination by the wave velocity method. University of Calif., IER., Series 74, Issue 6, September 1953.
3. Mathewson, W. W. - A manual for wave form analysis, Navy Dept., David Taylor Model Basin, Report No. 794, 1952.
4. Moffitt, F.H. - Analysis of non-uniform short-crested ocean waves for depth determination, based on wave velocity method, from timed vertical photographs taken over Clatsop Spit, Oregon. University of Calif., IER., Series 74, Issue 2, September 1953.
5. Stokes, J.J. - Surface waves in water of variable depth. Quart. Jour. Appl. Math. 5(1), 32 (1947)
6. Watson, G. N. - A treatise on the theory of Bessel functions. Cambridge University Press 1952.
7. Johnson, J. W. - Wave length on a sloping bottom. University of Calif. HE-116-15, May 1944.
8. Fuchs, R.A. - On the theory of short-crested oscillatory waves. Symp. on Gravity Waves at the National Bu. Stand., 1951, p 187.
9. Side, E.A. and Panton, R.H. - The modification of wave patterns in shallow water. Ministry of Supply, Wave Report No. 15, 1946.

Table 1

Table of Functions $S\left(\frac{h}{L_0}\right) = \int_{\frac{h}{L_0}}^{\frac{1}{2}} \frac{d\left(\frac{h}{L_0}\right)}{\frac{h}{L_0}}$ and $R\left(\frac{h}{L_0}\right) = \int_{\frac{h}{L_0}}^{\frac{1}{2}} \frac{\frac{h}{L_0} d\left(\frac{h}{L_0}\right)}{\frac{h}{L_0}}$

| $\frac{h}{L_0}$ | $S\left(\frac{h}{L_0}\right)$ | $R\left(\frac{h}{L_0}\right)$ | $\frac{h}{L_0}$ | $S\left(\frac{h}{L_0}\right)$ | $R\left(\frac{h}{L_0}\right)$ | $\frac{h}{L_0}$ | $S\left(\frac{h}{L_0}\right)$ | $R\left(\frac{h}{L_0}\right)$ |
|-----------------|-------------------------------|-------------------------------|-----------------|-------------------------------|-------------------------------|-----------------|-------------------------------|-------------------------------|
| .50 | 0 | 0 | .115 | .41370 | .12406 | .025 | .56876 | .13419 |
| .49 | 0.01004 | .00498 | .110 | .42044 | .12482 | .024 | .57137 | .13426 |
| .48 | 0.02008 | .00984 | .105 | .42729 | .12555 | .023 | .57404 | .13432 |
| .47 | 0.03013 | .01461 | .100 | .43427 | .12626 | .022 | .57677 | .13438 |
| .46 | 0.04019 | .01929 | .098 | .43710 | .12654 | .021 | .57955 | .13443 |
| .45 | 0.05025 | .02387 | .096 | .43995 | .12683 | .020 | .58240 | .13450 |
| .44 | 0.06033 | .02835 | .094 | .44283 | .12709 | .019 | .58532 | .13454 |
| .43 | 0.07041 | .03274 | .092 | .44573 | .12737 | .018 | .58831 | .13461 |
| .42 | 0.08050 | .03703 | .090 | .44866 | .12764 | .017 | .59139 | .13466 |
| .41 | 0.09060 | .04122 | .088 | .45161 | .12796 | .016 | .59455 | .13471 |
| .40 | 0.10072 | .04531 | .086 | .45458 | .12816 | .015 | .59781 | .13477 |
| .39 | 0.11085 | .04933 | .084 | .45759 | .12842 | .014 | .60117 | .13482 |
| .38 | 0.12100 | .05323 | .082 | .46063 | .12867 | .013 | .60465 | .13486 |
| .37 | 0.13117 | .05704 | .080 | .46369 | .12891 | .012 | .60827 | .13491 |
| .36 | 0.14136 | .06076 | .078 | .46679 | .12915 | .011 | .61204 | .13495 |
| .35 | 0.15157 | .06439 | .076 | .46991 | .12941 | .010 | .61598 | .13499 |
| .34 | 0.16181 | .06742 | .074 | .47308 | .12963 | .009 | .62011 | .13503 |
| .33 | 0.17207 | .071353 | .072 | .47627 | .12987 | .008 | .62448 | .13507 |
| .32 | 0.18238 | .07470 | .070 | .47951 | .13010 | .007 | .62912 | .13510 |
| .31 | 0.19272 | .07796 | .068 | .48279 | .13033 | .006 | .63411 | .13514 |
| .30 | 0.20310 | .08113 | .066 | .48610 | .13056 | .005 | .63962 | .13517 |
| .29 | 0.21352 | .08420 | .064 | .48946 | .13077 | .0045 | .64253 | .13518 |
| .28 | 0.22400 | .08719 | .062 | .49287 | .13099 | .0040 | .64561 | .13520 |
| .27 | 0.23454 | .09010 | .060 | .49632 | .13120 | .0035 | .64888 | .13521 |
| .26 | 0.24515 | .09290 | .058 | .49982 | .13139 | .0030 | .65240 | .13522 |
| .25 | 0.25582 | .09563 | .056 | .50338 | .13161 | .0025 | .65623 | .13523 |
| .24 | 0.26658 | .09826 | .054 | .50699 | .13181 | .0023 | .65786 | .13523 |
| .23 | 0.27743 | .10081 | .052 | .51066 | .13199 | .0021 | .65957 | .13524 |
| .22 | 0.28838 | .10328 | .050 | .51439 | .13219 | .0019 | .66135 | .13524 |
| .210 | 0.29944 | .10565 | .048 | .51819 | .13238 | .0017 | .66324 | .13524 |
| .205 | 0.30502 | .10681 | .046 | .52207 | .13255 | .0015 | .66524 | .13525 |
| .200 | 0.31063 | .10794 | .044 | .52502 | .13274 | .0014 | .66629 | .13525 |
| .195 | 0.31627 | .10906 | .042 | .53005 | .13290 | .0013 | .66737 | .13525 |
| .190 | 0.32196 | .11016 | .040 | .53416 | .13307 | .0012 | .66851 | .13525 |
| .185 | 0.32768 | .11123 | .039 | .53626 | .13315 | .0011 | .66969 | .13525 |
| .180 | 0.33345 | .11228 | .038 | .53838 | .13324 | .0010 | .67092 | .13525 |
| .175 | 0.33926 | .11331 | .037 | .54052 | .13332 | .0009 | .67222 | .13525 |
| .170 | 0.34511 | .11433 | .036 | .54269 | .13340 | .0008 | .67334 | .13525 |
| .165 | 0.35102 | .11532 | .035 | .54489 | .13347 | .0007 | .67504 | .13526 |
| .160 | 0.35698 | .11629 | .034 | .54712 | .13355 | .0006 | .67661 | .13526 |
| .155 | 0.36300 | .11723 | .033 | .54938 | .13363 | .0005 | .67832 | .13526 |
| .150 | 0.36907 | .11816 | .032 | .55167 | .13370 | .0004 | .68020 | .13526 |
| .145 | 0.37522 | .11906 | .031 | .55400 | .13378 | .0003 | .68234 | .13526 |
| .140 | 0.38143 | .11975 | .030 | .55636 | .13385 | .0002 | .68488 | .13526 |
| .135 | 0.38771 | .12082 | .029 | .55876 | .13392 | .0001 | .68818 | .13526 |
| .130 | 0.39407 | .12166 | .028 | .56119 | .13398 | .0000 | .69616 | .13526 |
| .125 | 0.40052 | .12248 | .027 | .56367 | .13406 | | | |
| .120 | 0.40706 | .12328 | .026 | .56619 | .13412 | | | |

TABLE II

COMPARISON OF TRUE AND COMPUTED DEPTHS FOR STRAIGHT BEACHES OF SLOPE α

$$\alpha = 1/40$$

| T = 20 | | T = 15 | | T = 10 | | T = 5 | |
|-----------|---------------|-----------|---------------|-----------|---------------|-----------|---------------|
| True d | Computed d | True d | Computed d | True d | Computed d | True d | Computed d |
| 1024.0 | 1024.0 | 576.0 | 576.0 | 256.0 | 256.0 | 64.0 | 64.0 |
| 970.8 | 973.0 | 546.0 | 547.3 | 242.7 | 243.3 | 60.7 | 60.8 |
| 915.5 | 922.1 | 514.4 | 518.7 | 228.9 | 230.5 | 57.2 | 57.6 |
| 868.4 | 871.3 | 488.4 | 490.1 | 217.1 | 217.8 | 54.3 | 54.5 |
| 817.2 | 820.7 | 459.6 | 461.6 | 204.3 | 205.2 | 51.1 | 51.3 |
| 766.0 | 770.2 | 430.8 | 433.2 | 191.5 | 192.5 | 47.9 | 48.1 |
| 718.8 | 720.0 | 404.4 | 405.0 | 179.7 | 180.0 | 44.9 | 45.0 |
| 667.6 | 670.0 | 375.6 | 376.9 | 166.9 | 167.5 | 41.7 | 41.9 |
| 619.5 | 620.5 | 348.5 | 349.0 | 154.9 | 155.1 | 38.7 | 38.9 |
| 570.4 | 571.5 | 320.8 | 321.5 | 142.6 | 142.9 | 35.6 | 35.7 |
| 520.6 | 523.2 | 292.8 | 294.3 | 130.2 | 130.8 | 32.5 | 32.7 |
| 473.9 | 475.6 | 266.6 | 267.5 | 118.5 | 118.9 | 29.6 | 29.7 |
| 427.6 | 429.1 | 240.5 | 241.3 | 106.9 | 107.3 | 26.7 | 26.8 |
| 382.2 | 383.7 | 215.0 | 215.8 | 95.5 | 95.9 | 23.9 | 24.0 |
| 338.2 | 339.7 | 190.2 | 191.1 | 84.5 | 84.9 | 21.1 | 21.2 |
| 296.3 | 297.3 | 166.7 | 167.2 | 74.1 | 74.3 | 18.5 | 18.6 |
| 255.6 | 256.8 | 143.8 | 144.5 | 63.9 | 64.2 | 16.0 | 16.1 |
| 217.3 | 218.5 | 122.3 | 122.9 | 54.3 | 54.6 | 13.6 | 13.7 |
| 181.3 | 182.5 | 102.0 | 102.6 | 45.3 | 45.6 | 11.3 | 11.4 |
| 148.0 | 149.1 | 83.2 | 83.9 | 37.0 | 37.3 | 9.2 | 9.3 |
| 117.4 | 118.6 | 66.0 | 66.7 | 29.4 | 29.6 | 7.3 | 7.4 |
| 90.1 | 91.2 | 50.7 | 51.3 | 22.5 | 22.8 | 5.6 | 5.7 |
| 66.0 | 67.0 | 37.1 | 37.7 | 16.5 | 16.8 | 4.1 | 4.2 |
| 45.3 | 46.4 | 25.5 | 26.1 | 11.3 | 11.6 | 2.8 | 2.9 |
| 28.3 | 29.4 | 15.9 | 16.5 | 7.1 | 7.3 | 1.8 | 1.8 |
| 15.1 | 16.2 | 8.5 | 9.1 | 3.8 | 4.0 | 0.9 | 1.0 |
| 5.9 | 6.8 | 3.3 | 3.8 | 1.5 | 1.7 | 0.4 | 0.4 |

$$\alpha = 1/100$$

| | | | | | | | |
|--------|--------|-------|-------|-------|-------|------|------|
| 1024.0 | 1024.0 | 576.0 | 576.0 | 256.0 | 256.0 | 64.0 | 64.0 |
| 1007.6 | 1003.6 | 566.8 | 564.5 | 251.9 | 250.9 | 63.0 | 62.7 |
| 987.1 | 983.2 | 555.3 | 553.1 | 246.8 | 245.8 | 61.7 | 61.5 |
| 954.4 | 952.8 | 536.3 | 541.6 | 238.6 | 240.7 | 59.6 | 60.2 |
| 940.0 | 942.5 | 528.8 | 530.1 | 235.0 | 235.6 | 58.8 | 58.9 |
| 915.5 | 922.1 | 514.9 | 518.7 | 228.9 | 230.5 | 57.2 | 57.6 |
| 892.9 | 901.8 | 502.3 | 507.3 | 223.2 | 225.4 | 55.8 | 56.4 |
| 882.7 | 881.5 | 496.5 | 495.8 | 220.7 | 220.4 | 55.2 | 55.1 |
| 872.4 | 861.2 | 490.8 | 484.4 | 218.1 | 215.3 | 54.5 | 53.8 |
| 845.8 | 840.9 | 475.8 | 473.0 | 211.5 | 210.2 | 52.9 | 52.6 |
| 816.1 | 820.7 | 459.1 | 461.6 | 204.0 | 205.2 | 51.0 | 51.3 |
| 796.7 | 800.4 | 448.1 | 450.2 | 199.2 | 200.1 | 49.8 | 50.0 |
| 778.2 | 780.3 | 437.8 | 438.9 | 194.6 | 195.1 | 48.6 | 48.8 |
| 761.7 | 760.1 | 428.5 | 427.6 | 190.5 | 190.0 | 47.6 | 47.5 |
| 716.8 | 720.0 | 403.2 | 405.0 | 179.2 | 180.0 | 44.8 | 45.0 |
| 701.8 | 699.9 | 394.8 | 393.7 | 175.5 | 175.0 | 43.9 | 43.7 |
| 680.6 | 680.0 | 382.8 | 382.5 | 170.1 | 170.0 | 42.5 | 42.5 |
| 658.8 | 660.1 | 370.6 | 371.3 | 164.7 | 165.0 | 41.2 | 41.3 |
| 639.0 | 640.3 | 359.4 | 360.1 | 159.7 | 160.0 | 39.9 | 40.0 |
| 621.0 | 620.5 | 349.3 | 349.0 | 155.2 | 155.1 | 38.8 | 38.8 |

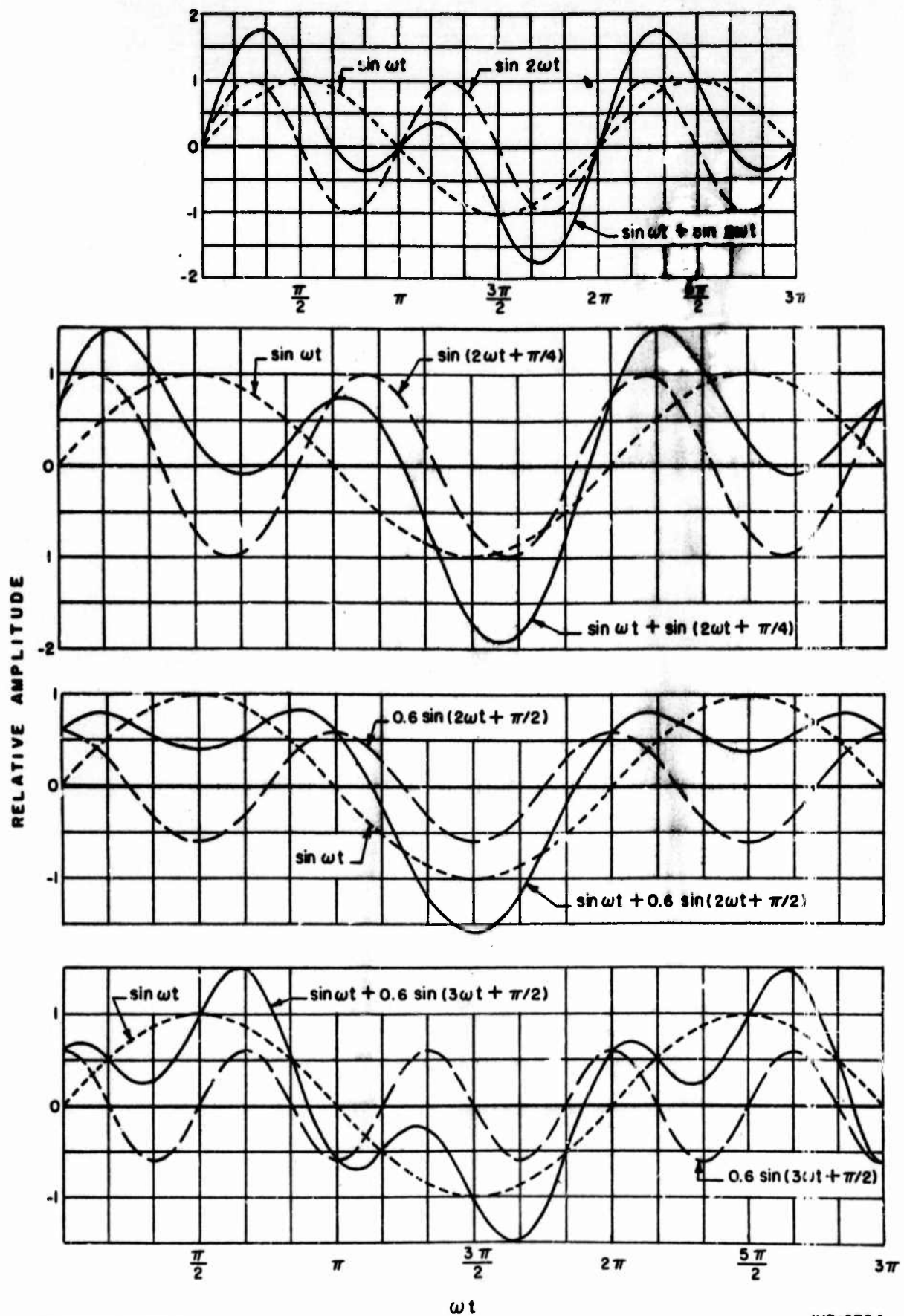
Table II cont'd.

| T = 20 | | T = 15 | | $\alpha = 1/100$ T = 10 | | T = 5 | |
|-----------|---------------|-----------|---------------|----------------------------|---------------|-----------|---------------|
| True d | Computed d | True d | Computed d | True d | Computed d | True d | Computed d |
| 602.1 | 600.8 | 338.7 | 338.0 | 150.5 | 150.2 | 37.6 | 37.6 |
| 580.8 | 581.3 | 326.7 | 327.0 | 145.2 | 145.3 | 36.3 | 36.3 |
| 561.5 | 561.8 | 315.8 | 316.0 | 140.4 | 140.4 | 35.1 | 35.1 |
| 542.4 | 542.4 | 305.1 | 305.1 | 135.6 | 135.6 | 33.9 | 33.9 |
| 521.6 | 523.2 | 293.4 | 294.3 | 130.4 | 130.8 | 32.6 | 32.7 |
| 502.8 | 504.1 | 282.8 | 283.5 | 125.7 | 126.0 | 31.4 | 31.5 |
| 485.4 | 485.1 | 273.0 | 272.9 | 121.3 | 121.3 | 30.3 | 30.3 |
| 447.6 | 447.6 | 251.8 | 251.8 | 111.9 | 111.9 | 28.0 | 28.0 |
| 429.9 | 429.1 | 241.8 | 241.3 | 107.5 | 107.3 | 26.9 | 26.8 |
| 410.7 | 410.7 | 231.0 | 231.0 | 102.7 | 102.7 | 25.7 | 25.7 |
| 392.2 | 392.6 | 220.6 | 220.9 | 98.0 | 98.2 | 24.5 | 24.5 |
| 374.0 | 374.8 | 210.4 | 210.8 | 93.5 | 93.7 | 23.4 | 23.4 |
| 357.4 | 357.1 | 201.0 | 200.9 | 89.3 | 89.3 | 22.3 | 22.3 |
| 339.6 | 339.7 | 191.0 | 191.1 | 84.9 | 84.9 | 21.2 | 21.2 |
| 322.3 | 322.5 | 181.3 | 181.4 | 80.6 | 80.6 | 20.1 | 20.2 |
| 305.5 | 305.6 | 171.9 | 171.9 | 76.4 | 76.4 | 19.1 | 19.1 |
| 288.6 | 289.1 | 162.3 | 162.6 | 72.1 | 72.3 | 18.0 | 18.1 |
| 273.3 | 272.8 | 153.7 | 153.4 | 68.3 | 68.2 | 17.1 | 17.0 |
| 256.4 | 256.8 | 144.2 | 144.4 | 64.1 | 64.2 | 16.0 | 16.1 |
| 240.9 | 241.2 | 135.5 | 135.7 | 60.2 | 60.3 | 15.1 | 15.1 |
| 226.3 | 226.0 | 127.3 | 127.1 | 56.6 | 56.5 | 14.1 | 14.1 |
| 211.4 | 211.1 | 118.9 | 118.7 | 52.8 | 52.8 | 13.2 | 13.2 |
| 196.7 | 196.5 | 110.6 | 110.6 | 49.2 | 49.1 | 12.3 | 12.3 |
| 182.3 | 182.5 | 102.6 | 102.6 | 45.6 | 45.6 | 11.4 | 11.4 |
| 168.9 | 168.8 | 95.0 | 94.9 | 42.2 | 42.2 | 10.6 | 10.6 |
| 155.3 | 155.5 | 87.4 | 87.5 | 38.8 | 38.9 | 9.7 | 9.7 |
| 142.5 | 142.7 | 80.2 | 80.3 | 35.6 | 35.7 | 8.9 | 8.9 |
| 130.3 | 130.4 | 73.3 | 73.4 | 32.6 | 32.6 | 8.1 | 8.1 |
| 118.3 | 118.6 | 66.5 | 66.7 | 29.6 | 29.6 | 7.4 | 7.4 |
| 106.9 | 107.2 | 60.1 | 60.3 | 26.7 | 26.8 | 6.7 | 6.7 |
| 96.1 | 96.4 | 54.1 | 54.2 | 24.0 | 24.1 | 6.0 | 6.0 |
| 86.1 | 86.1 | 48.4 | 48.4 | 21.5 | 21.5 | 5.4 | 5.4 |
| 76.2 | 76.3 | 42.9 | 42.9 | 19.0 | 19.1 | 4.8 | 4.8 |
| 66.8 | 67.0 | 37.6 | 37.7 | 16.7 | 16.8 | 4.2 | 4.2 |
| 58.3 | 58.3 | 32.8 | 32.8 | 14.6 | 14.6 | 3.6 | 3.6 |
| 50.1 | 50.2 | 28.2 | 28.2 | 12.5 | 12.6 | 3.1 | 3.1 |
| 42.4 | 42.7 | 23.9 | 24.0 | 10.6 | 10.7 | 2.7 | 2.7 |
| 35.5 | 35.7 | 20.0 | 20.1 | 8.9 | 8.9 | 2.2 | 2.2 |
| 29.2 | 29.4 | 16.4 | 16.5 | 7.3 | 7.3 | 1.8 | 1.8 |
| 23.5 | 23.6 | 13.2 | 13.3 | 5.9 | 5.9 | 1.5 | 1.5 |
| 18.3 | 18.5 | 10.3 | 10.4 | 4.6 | 4.6 | 1.1 | 1.2 |
| 13.7 | 13.7 | 7.7 | 7.9 | 3.4 | 3.5 | 0.86 | 0.87 |
| 9.8 | 10.1 | 5.5 | 5.7 | 2.5 | 2.5 | 0.61 | 0.63 |
| 6.6 | 6.8 | 3.7 | 3.8 | 1.6 | 1.7 | 0.41 | 0.43 |
| 4.0 | 4.2 | 2.3 | 2.4 | 1.0 | 1.0 | 0.25 | 0.26 |
| 1.99 | 2.19 | 1.12 | 1.23 | 0.50 | 0.55 | 0.12 | 0.14 |
| 0.63 | 0.84 | 0.36 | 0.47 | 0.16 | 0.21 | 0.04 | 0.05 |

TABLE III

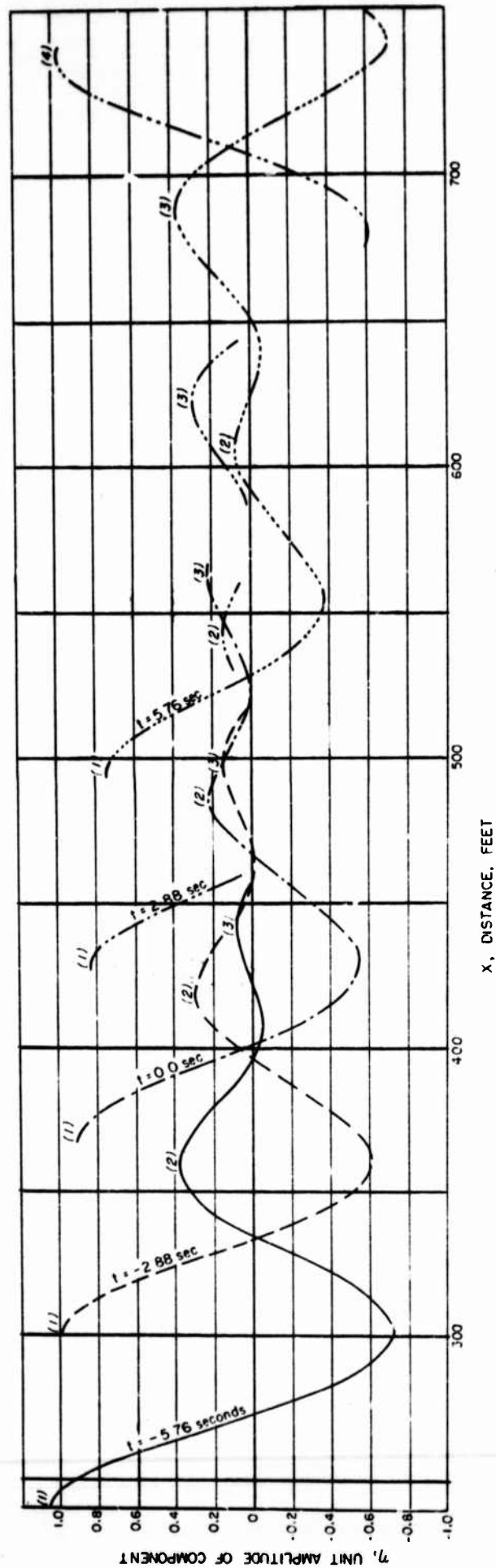
COMPARISON OF TRUE AND COMPUTED DEPTHS FOR A PARABOLIC BEACH

| T = 5 sec. | | T = 10 sec. | | T = 15 sec. | | T = 20 sec. | |
|--------------------|------------------------|--------------------|------------------------|--------------------|------------------------|--------------------|------------------------|
| True depth d | Computed depth d | True depth d | Computed depth d | True depth d | Computed depth d | True depth d | Computed depth d |
| .4 | | 1.2 | | 3.6 | | 2.1 | |
| 1.3 | 1.1 | 4.3 | 3.8 | 10.0 | 9.1 | 10.3 | 8.7 |
| 2.7 | 2.8 | 8.6 | 8.1 | 17.4 | 16.6 | 20.3 | 19.4 |
| 4.4 | 3.4 | 13.3 | 12.9 | 24.8 | 23.9 | 30.3 | 28.6 |
| 6.4 | 6.3 | 18.1 | 17.9 | 32.0 | 30.7 | 39.5 | 38.4 |
| 8.5 | 8.5 | 23.0 | 23.0 | 38.9 | 38.8 | 48.9 | 48.7 |
| 10.7 | 10.6 | 27.8 | 27.9 | 46.0 | 47.0 | 57.6 | 55.5 |
| 12.9 | 12.6 | 32.5 | 32.1 | 52.5 | 51.8 | 65.9 | 67.5 |
| 15.1 | 15.1 | 37.0 | 36.4 | 58.9 | 58.9 | 74.3 | 73.8 |
| 17.3 | 17.4 | 41.4 | 41.2 | 65.1 | 65.7 | 81.9 | 80.8 |
| 19.5 | 19.2 | 45.6 | 45.3 | 71.1 | 72.1 | 89.7 | 92.1 |
| 21.6 | 21.5 | 49.8 | 49.8 | 77.0 | 75.9 | 97.1 | 100.3 |
| 23.7 | 23.6 | 53.9 | 54.1 | 82.5 | 81.3 | 102.4 | 104.2 |
| 25.7 | 25.5 | 57.9 | 57.1 | 88.0 | 86.8 | 111.2 | 106.8 |
| 27.6 | 28.0 | 61.7 | 61.9 | 93.3 | 92.9 | 118.0 | 119.6 |
| 29.6 | 29.7 | 65.5 | 66.3 | 98.6 | 100.8 | 124.7 | 124.1 |
| 31.4 | 31.2 | 69.2 | 69.2 | 103.8 | 103.4 | 131.1 | 127.8 |
| 33.3 | 32.9 | 72.8 | 73.2 | 108.7 | 109.2 | 137.4 | 140.8 |
| 35.0 | 34.6 | 76.3 | 76.7 | 112.1 | 112.8 | 143.8 | 142.7 |
| 36.8 | 36.6 | 79.7 | 79.0 | 118.4 | 115.3 | 149.7 | 149.7 |
| 38.4 | 38.3 | 83.1 | 82.7 | 123.1 | 125.7 | 155.9 | 149.0 |
| 40.1 | 40.0 | 86.4 | 86.0 | 127.9 | 137.6 | 161.4 | 160.6 |
| 41.8 | 40.9 | 89.6 | 89.2 | 132.6 | 144.7 | 167.5 | 174.5 |
| 43.4 | 44.9 | 92.8 | 93.2 | 137.2 | 139.8 | 173.1 | 157.6 |
| 44.9 | 45.5 | 95.9 | 97.2 | 141.6 | 136.8 | 178.4 | 146.0 |
| 46.5 | 43.8 | 99.0 | 97.5 | 145.8 | 138.1 | 183.3 | 181.6 |
| 48.0 | 45.3 | 101.9 | 99.6 | 150.0 | 142.1 | 189.4 | 231.9 |
| 49.4 | 51.7 | 107.5 | 105.8 | 154.1 | 152.7 | 195.0 | 197.2 |
| 50.9 | 51.0 | 107.8 | | 153.2 | 154.1 | 200.1 | |
| 52.3 | 52.4 | | | 162.3 | 157.7 | | |
| 53.7 | 59.7 | | | 166.3 | 171.2 | | |
| 55.0 | 52.4 | | | 170.0 | 183.2 | | |
| 56.4 | 51.0 | | | 174.4 | 177.2 | | |
| 57.7 | 61.3 | | | | | | |
| 59.0 | | | | | | | |
| 60.3 | 57.1 | | | | | | |
| 61.5 | 57.1 | | | | | | |
| 62.8 | 52.5 | | | | | | |



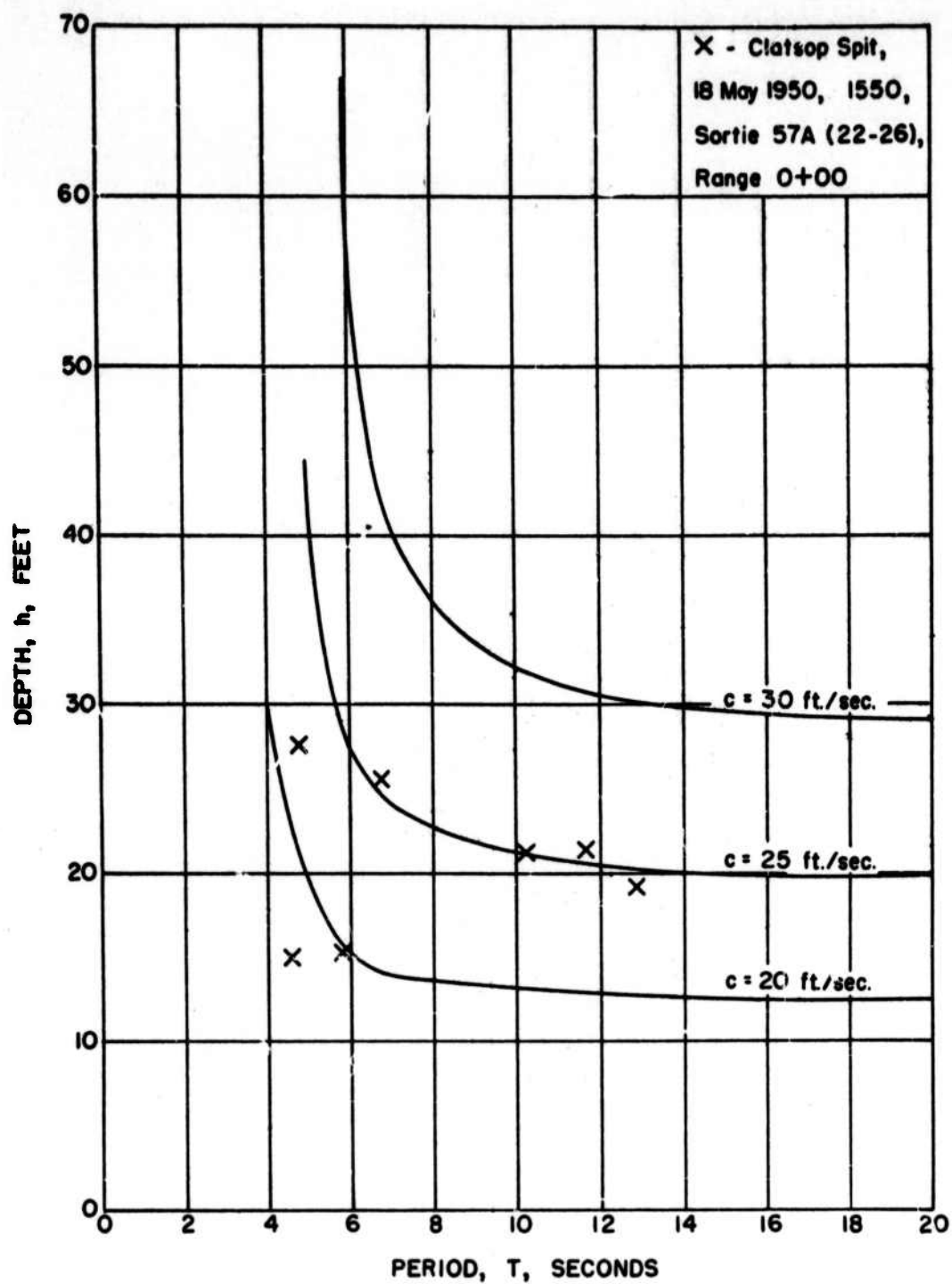
HYD-6784

COMBINATIONS OF FUNDAMENTAL AND HIGHER HARMONIC WAVE FORMS



HYD-6785

SURFACE PROFILES OF THE SUM OF TWO SINUSOIDAL WAVES AT VARIOUS TIMES



**WATER DEPTH VERSUS WAVE PERIOD
WITH WAVE VELOCITY AS A PARAMETER**

HYD-8786

FIGURE 3

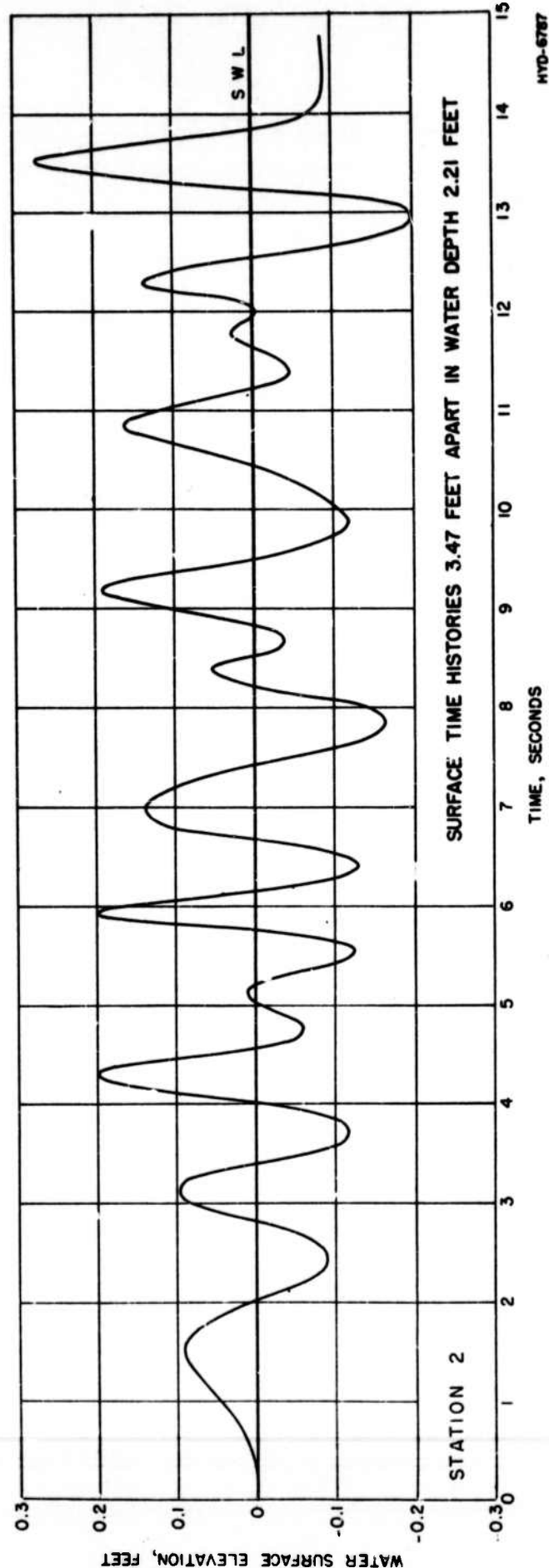
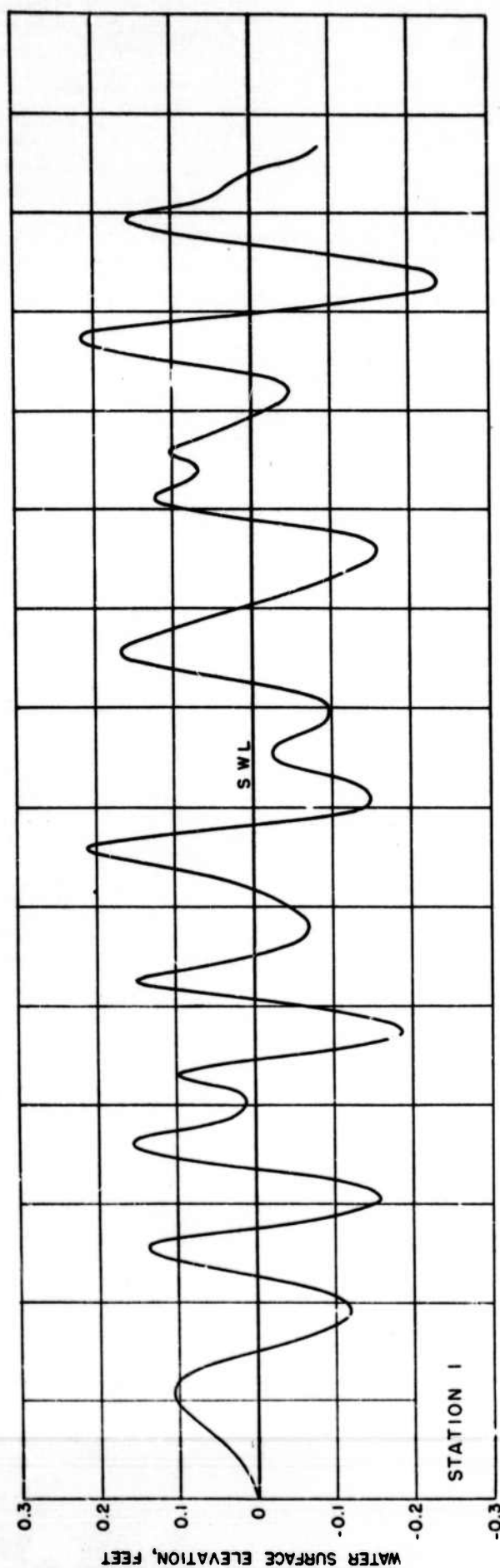


FIGURE 4

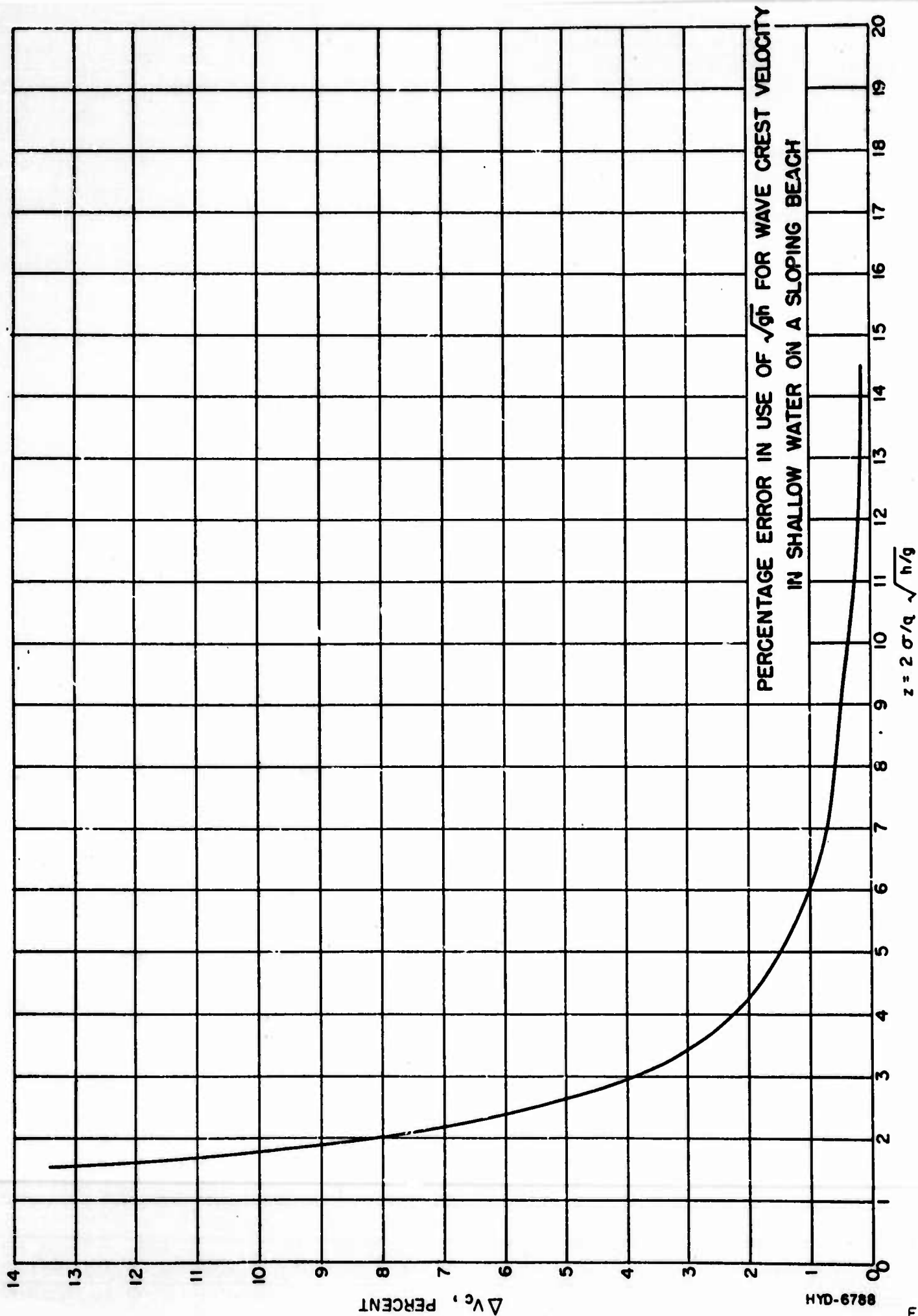
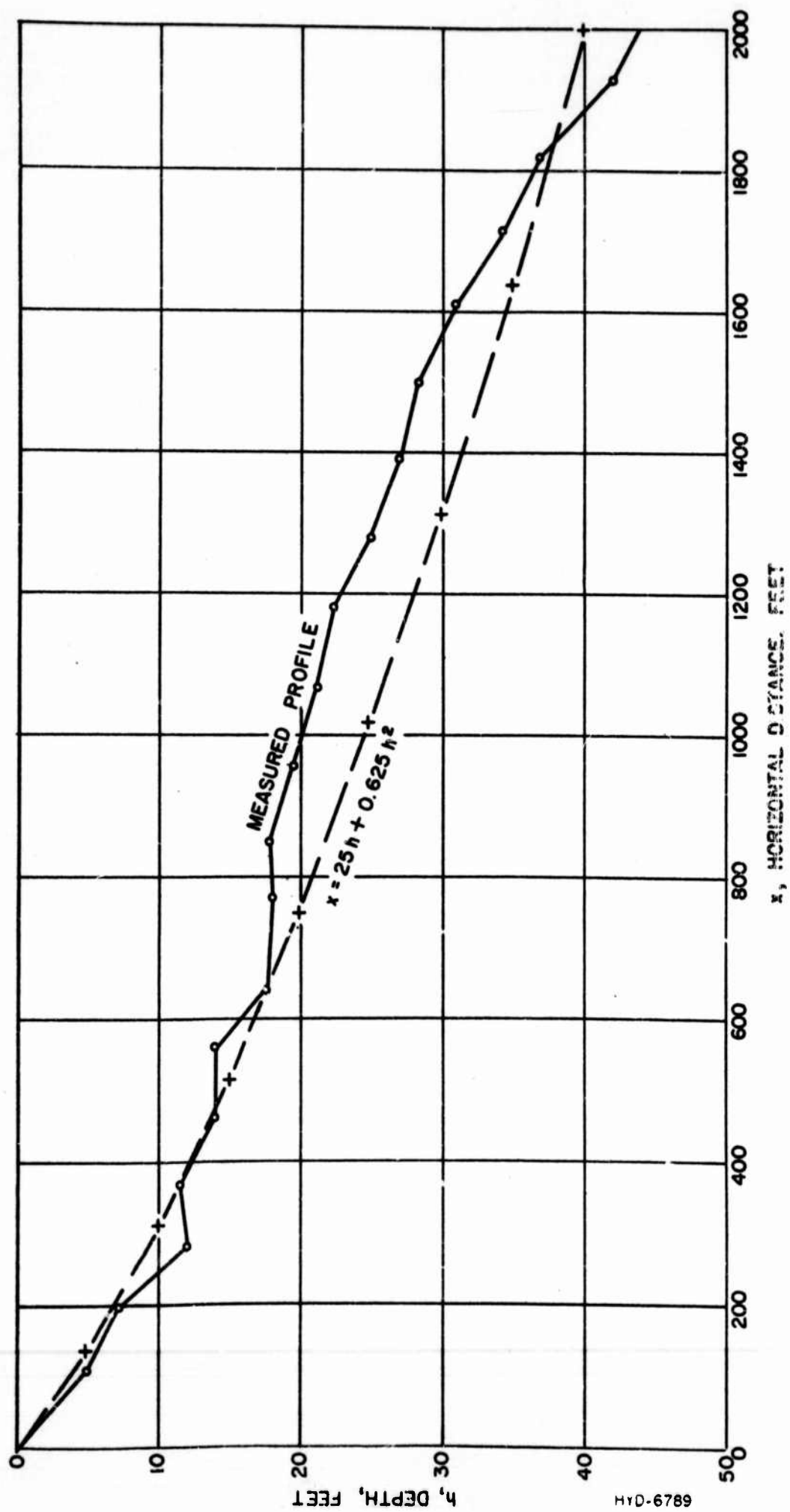
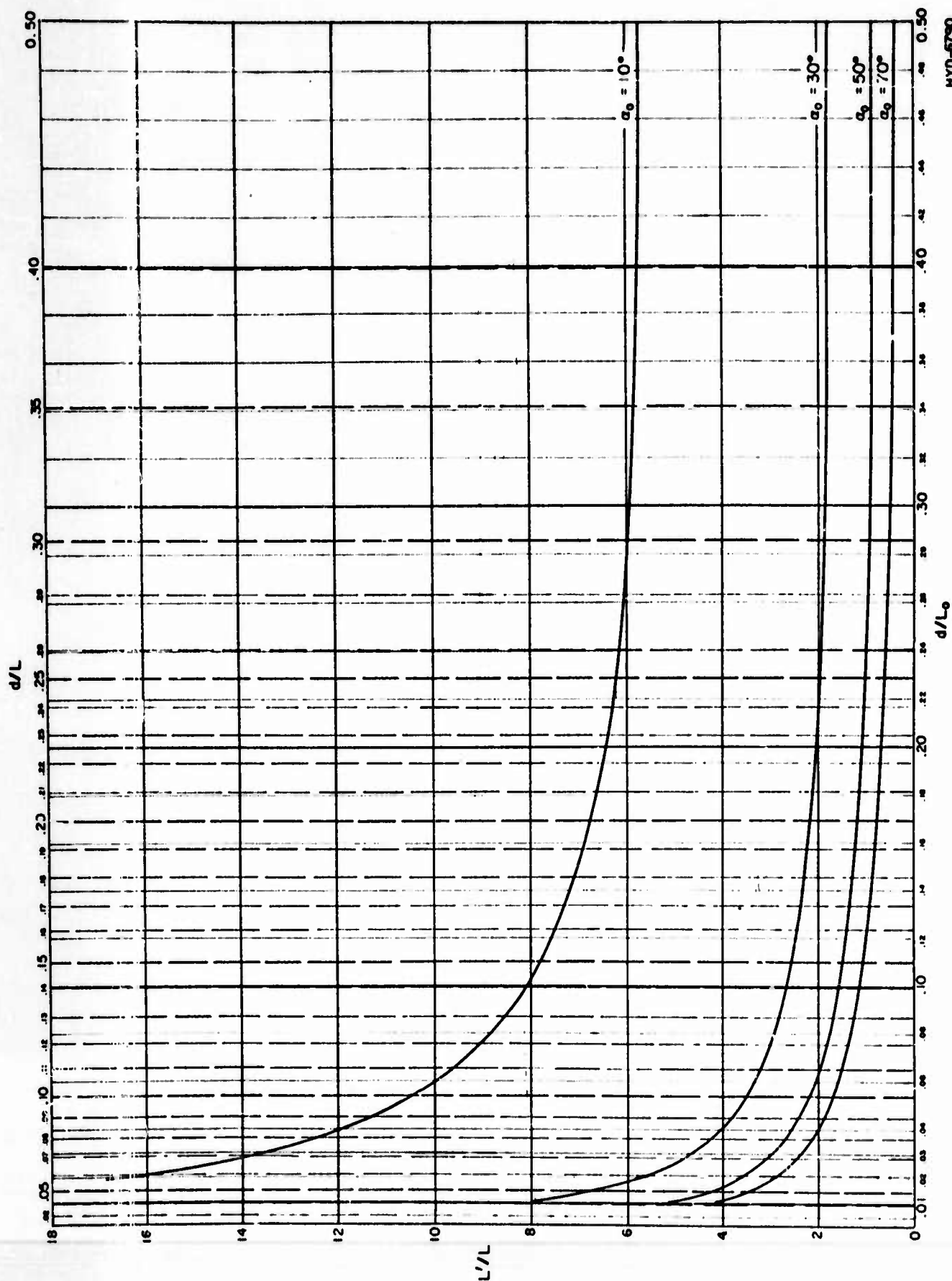


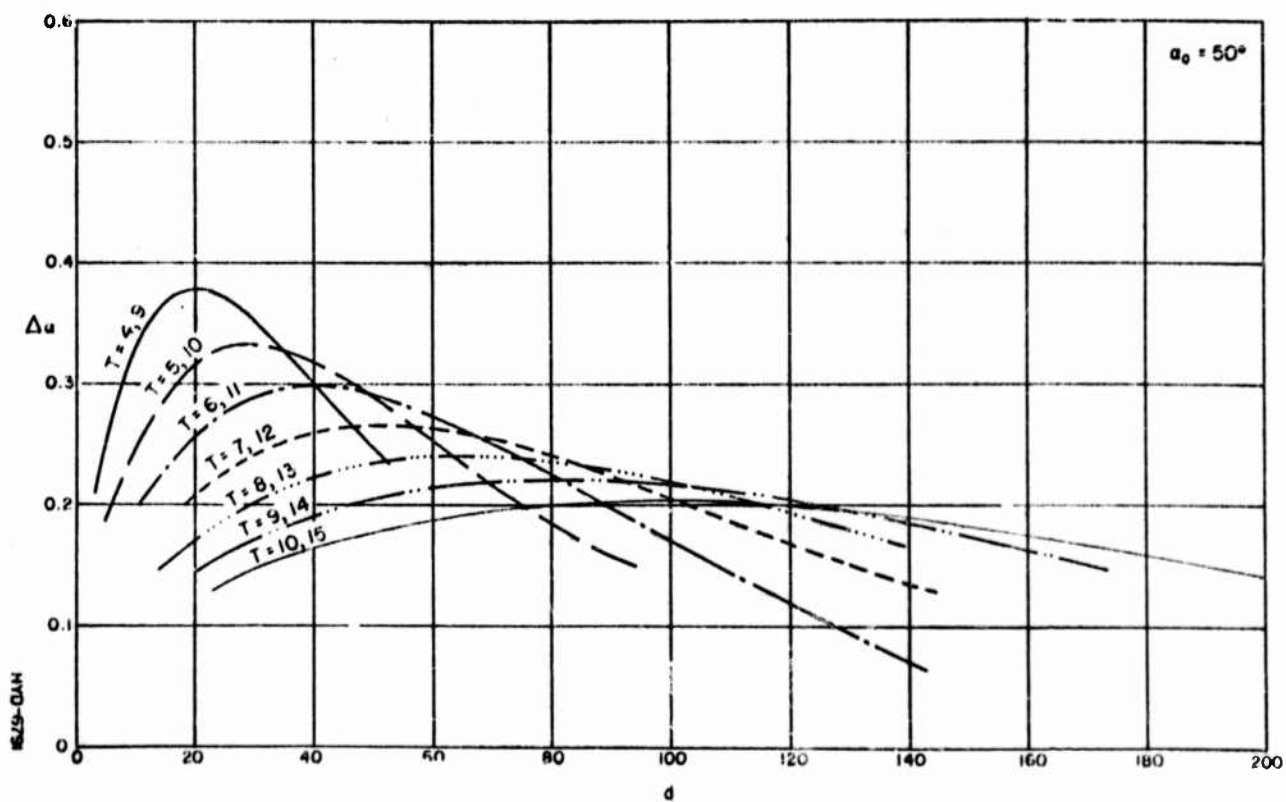
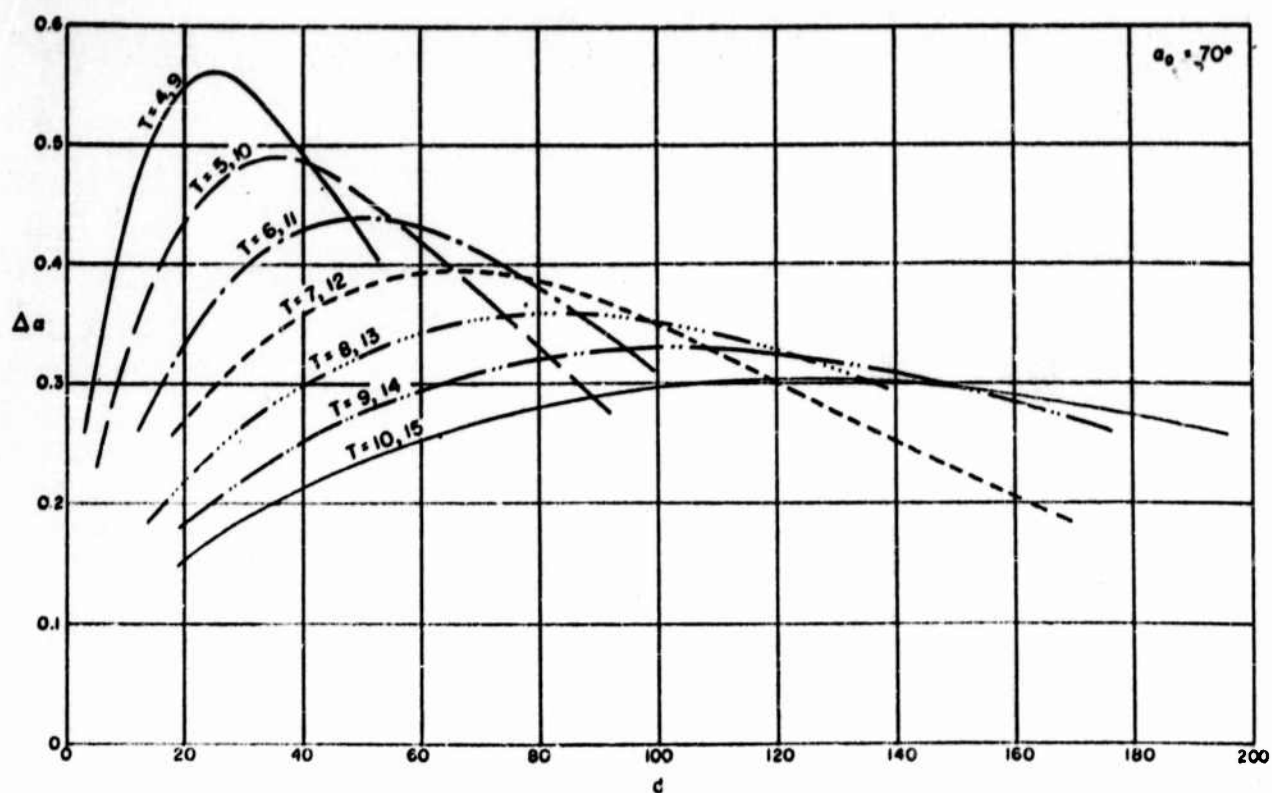
FIG. 5



MEASURED AND ASSUMED BEACH PROFILE, DAVENPORT, CALIFORNIA



WAVE LENGTH RATIO, L'/L , VERSUS d/L_0 FOR VARIOUS INITIAL REFRACTION ANGLES
OF A SHORT-CRESTED WAVE APPROACHING THE BEACH AT RIGHT ANGLES



ANGULAR DIVERGENCE OF CRESTS OF TWO WAVES OF DIFFERENT PERIODS
APPROACHING THE BEACH AT AN ACUTE ANGLE

DISTRIBUTION LIST
Unclassified Technical Reports

| Copies | Addressee | Copies | Addressee |
|--------|--|--------|---|
| 13 | Director Inst. of Engineering Research University of California Berkeley 4, Calif. | 1 | Asst. Secty of Defense for Research and Development Attn: Comm. on Geophys. & Geography Pentagon Bldg. Washington 25, D.C. |
| 1 | Chief of Naval Operations Navy Dept. Attn: Op-533D Washington 25, D.C. | 2 | Asst. Naval Attache for Res. American Embassy Navy No. 100 FPO, New York, N.Y. |
| 2 | Geophysics Branch, Code 416 Office of Naval Research Washington 25, D.C. | 2. | U.S. Bureau of Ships Navy Dept. Washington 25, D.C. Attn: Code 847 |
| 6 | Director, Naval Research Lab. Attn: Tech. Information Officer Washington 25, D.C. | 1 | Commander Naval Ord. Lab. White Oak Silver Springs, Md. |
| 2 | Officer-in-Charge Office of Naval Research, London Br. Navy No. 100 FPO. New York, N.Y. | 1 | Commanding General, Res. & Devel. Dept of the Air Force Washington 25, D.C. |
| 1 | Office of Naval Research Branch Office 346 Broadway New York, 13, N.Y. | 1 | Chief of Naval Research Navy Dept. Code 466 Washington 25, D.C. |
| 1 | Office of Naval Research, Branch Office 10th Floor, The John Crerar Library 86 E. Randolph St. Chicago, Ill. | 8 | U.S. Navy Hydrographic Office Washington 25, D.C. Attn: Div. of Oceanography |
| 1 | Office of Naval Research, Br. Off. 1030 East Green St. Pasadena, 1, Calif. | 2 | Director U.S. Navy Electronics Lab. San Diego 52, Calif. Attn: Codes 550, 552 |
| 1 | ONR. Branch Office 1000 Geary St. San Francisco, Calif. | 1 | Chief Bu. Yards and Docks Navy Dept. Washington 25, D.C. |
| 1 | ONR. Resident Representative University of Calif. T-3 | 1 | Commanding General Research and Development Div. Dept. of the Army Washington 25, D.C. |
| 1 | Office of Technical Services Dept of Commerce Washington 25, D.C. | 1 | Commanding Officer Air Force Comb. Research & Development Center CRQST-2 230 Albany St. Cambridge 39, Mass. |
| 5 | Armed Services Tech. Information Center Documents Service Center Knott Bldg, Dayton 2, Ohio. | | |

| Copies | Addressee | Copies | Addressee |
|--------|---|--------|---|
| 1 | Project AROWA, U.S. Naval Air Sta. Bldg R-48 Norfolk, Virginia | 1 | Allen Hancock Foundation University of Southern Calif. Los Angeles 7, Calif. |
| 1 | Dept of Aerology U.S. Naval Post Graduate School Monterey, California. | 1 | Director Narragansett Marine Lab. Kingston, R.I. |
| 1 | Commandant (OAO), U.S. Coast Guard 1300 E. St. N.W. Washington 25, D.C. | 1 | Director Chesapeake Bay Inst. Box 426 A RFD #2 Annapolis, Md. |
| 1 | Director, U.S. Coast and Geodetic Survey Dept of Commerce Washington 25, D.C. | 1 | Head, Dept. of Oceanography Texas A & M College College Station, Texas |
| 1 | U.S. Army, Beach Erosion Board 5201 Little Falls Rd. N.W. Washington 16, D.C. | 1 | Dr. Willard J. Pierson New York University University Heights New York 53, N.Y. |
| 1 | Dept of the Army Office of the Chief of Engineers Attn: Library Washington 25, D.C. | 1 | Director Hawaii Marine Lab. University of Hawaii Honolulu, T.H. |
| 1 | Mr. A.L. Cochran Chief, Hydrology and Hydr. Branch U.S. Corps of Engrs. Gravelly Point, Washington, D.C. | 1 | Director Marine Lab., University of Miami Coral Gables, Fla. |
| 1 | Commanding Officer U.S. Naval CE-Res. and Evaluation Lab. Construction Battn.Center Port Hueneme, Calif. | 1 | Head, Dept of Oceanography Brown University Providence, R.I. |
| 1 | Dept. of Engineering University of Calif. Berkeley, Calif. | 1 | Dept of Zoology Attn: Dr. H. Haskins Rutgers University New Brunswick, N.J. |
| 1 | The Oceanographic Inst. Florida State University Tallahassee, Florida | 2 | Library Scripps Inst. of Oceanography La Jolla, Calif. |
| 1 | Head, Dept. of Oceanography University of Washington Seattle, Washington | 2 | Director Woods Hole Oceanographic Inst. Woods Hole, Mass. |
| 1 | Bingham Oceanographic Foundation Yale University, New Haven, Connecticut | 2 | Director U.S. Fish and Wildlife Serv. Dept of the Interior Attn: Dr. L.A. Walford Washington 25, D.C. |
| 1 | Dept. of Conservation Cornell University Ithaca, N.Y. Attn: Dr. J. Ayers | 1 | U.S. Fish and Wildlife Serv. P.O. Box 3830 Honolulu, T.H. |
| 1 | Director, Lamont Geological Observ. Torrey Cliff Palisades, N.Y. | | |

| Copies | Addressee |
|--------|--|
| 1 | U.S. Fish and Wildlife Serv. Woods Hole, Mass. |
| 1 | U.S. Fish and Wildlife Serv. Fort Crockett, Galveston, Texas |
| 1 | U.S. Fish and Wildlife Serv. 450 B. Jordan Hall Stanford University Stanford, Calif. |
| 1 | U.S. Waterways Experiment Station Vicksburg, Miss. |
| 1 | U.S. Engineers Office San Francisco Dist. 180 New Montgomery St. San Francisco 19, Calif. |
| 1 | U.S. Engineers Office Los Angeles Dist. P.O. Box 17277, Foy Station Los Angeles 17, Calif. |
| 1 | Office of Honolulu Area Engrs. P.O. Box 2240 Honolulu, T.H. |
| 1 | Chairman, Ship to Shore Cont. Bd. U.S. Atlantic Fleet Commander Amphib. Group 2 FPO, N.Y., N.Y. |
| 1 | Commander, Amphibious Forces Pacific Fleet San Francisco, Calif. |
| 1 | Commander, Amphibious Training Command U.S. Pacific Fleet San Diego, 32, Calif. |
| 1 | Dr. M. St. Denis David Taylor Model Basin U.S. Navy Dept. Washington 25, D.C. |
| 1 | Dist. Engineer, Corps of Engrs. Jacksonville Dist. 575 Riverside Ave. Jacksonville, Fla. |
| 1 | Missouri River Division Corps of Engrs. U.S. Army P.O. Box 1216 Omaha 1, Nebraska |

| Copies | Addressee | 3. |
|--------|---|----|
| 1 | Commandant Marine Corps School Quantico, Va. | |
| 1 | Sir Claude Inglis, CBE. Division of Hydraulics Research % Office of Naval Research Navy No. 100 FPO. N.Y., N.Y. | |
| 1 | Commandant Hq. Marine Corps AO-4E Arlington Annex Washington, D.C. | |
| 1 | Chief, Andrews Air Force Base Washington 25, D.C. Attn: Mr. Stone | |
| 3 | U.S. Army Transportation Corps. Research and Development Fort Eustis, Va. Attn: Mr. J.R. Cloyd | |
| 3 | British Joint Services Mission Main Navy Bldg. Washington 25, D.C. | |
| 1 | California Academy of Sciences Golden Gate Park San Francisco, Calif. Attn: Dr. R.C. Miller. | |